

Comparative Lifetimes of Superdeformed Bands in $A \sim 80$ Nuclei

F. Lerma,⁽¹⁾ M. Devlin,⁽¹⁾ D. R. LaFosse,^(1,5) D. G. Sarantites,⁽¹⁾ R. M. Clark,⁽²⁾ I. Y. Lee,⁽²⁾
A. O. Macchiavelli,⁽²⁾ R. W. MacLeod,⁽²⁾ S. L. Tabor,⁽³⁾ D. Soltysik,⁽³⁾ C. Baktash⁽⁴⁾

⁽¹⁾ *Chemistry Department, Washington University, St. Louis, MO 63130*

⁽²⁾ *Nuclear Science Division, Lawrence Berkeley National Laboratory, Berkeley, CA 94720*

⁽³⁾ *Department of Physics, Florida State University, Tallahassee, FL 32306*

⁽⁴⁾ *Physics Division, Oak Ridge National Laboratory, Oak Ridge TN 37830*

⁽⁵⁾ *Current address: Department of Physics, SUNY at Stony Brook, Stony Brook, NY 11794*

Abstract. A comparative measurement of the transition quadrupole moments of the yrast superdeformed bands in $^{80-83}\text{Sr}$, ^{83}Y , ^{84}Zr has been performed using the Doppler-shift attenuation method. Thus, we have accurately measured the relative deformations of these structures, establishing for the first time, clear trends in the deformations of these bands. The yrast SD bands in the $^{80-83}\text{Sr}$ isotopes are shown to possess similar transition quadrupole moments, while significantly larger values are obtained for the ^{83}Y and ^{84}Zr cases. These results provide a stringent evaluation of the intruder orbital assignments of these structures, suggesting new assignments in some of these cases.

INTRODUCTION

Since the discovery of a discrete superdeformed (SD) band in ^{83}Sr [1,2], highly improved detection capabilities have allowed the study of a multitude of SD bands in several nuclei of mass ~ 80 . Superdeformed bands in these nuclei have been characterized as largely deformed prolate structures ($\beta_2 \sim 0.5$) due to their high spin nature, large dynamical moments of inertia ($\mathcal{J}^{(2)}$), and in various cases, from measured transition quadrupole moments (see for example, [3-7]). However, large experimental uncertainties have limited the accuracy of previous lifetime measurements, hampering clear estimates of the deformations of the SD bands in those nuclei. Consequently, well defined trends in the deformation of SD bands across the $A \sim 80$ nuclei have not been established.

In this work, we present the results from an experiment aimed to measure comparative transition quadrupole moments, Q_t , of the SD bands in $^{80-83}\text{Sr}$, ^{83}Y , and ^{84}Zr via the Doppler-shift attenuation method [8]. Recent lifetime measurements [3-7,9] have established that these bands are highly deformed ($\beta_2 \gtrsim 0.4$) prolate rotors. However, substantial variations in the systematic errors in those values hampered a clear understanding of the relative deformations of those bands. As a result, we have attempted to measure the deformations of those structures to establish clear comparisons with present intruder orbital assignments and to obtain trends in the evolution of superdeformation in these nuclei.

EXPERIMENTAL

The experiment was performed at the 88-inch Cyclotron at the Lawrence Berkeley National Laboratory. A single $570 \mu\text{g}/\text{cm}^2$ ^{58}Ni target foil backed with $3.2 \text{ mg}/\text{cm}^2$ of gold was used in two separate reactions. In the first reaction, the target was bombarded with a ^{28}Si beam at 130 MeV, populating high spin states in $^{80,82}\text{Sr}$, and ^{83}Y , via the $\alpha 2p$, $4p$ and $3p$ fusion-evaporation exit channels, respectively. In the second reaction, a ^{29}Si beam at 130 MeV was used to populate high-spin states in $^{81,83}\text{Sr}$, and ^{84}Zr via the $\alpha 2p$, $4p$ and $2pn$ exit channels, respectively. The γ rays emitted from the reactions were detected by the GAMMASPHERE array,

which consisted of 100 hyper-pure Ge detectors fitted with BGO Compton suppressors, and the residual charged particles were detected by the MICROBALL charged-particle detector array [10]. Each reaction was run for 2 days, accumulating $\sim 9 \times 10^8$ events per reaction. The hevimet absorber shields were removed during the experiment to obtain total γ -ray energy (H_γ), and γ fold (k_γ) information per event [11], and the event trigger was set to accept events with clean γ fold equal to 4 and higher. The MICROBALL provided good charged particle detection and identification, which were used to sort the data into individual exit channels. Residual contaminants in the particle gates resulting from unidentified protons, alpha particles and neutrons were sharply reduced by placing two-dimensional gates on H_γ and excitation energy, E^* (where, $E^* = \text{const.} - \Sigma \text{ particle energies}$) [12].

The energies of the charged particles detected with the MICROBALL were used to reconstruct the momenta of the recoiling nuclei on an event-by-event basis. These momenta were used to perform a precise Doppler-shift correction to the γ -ray energies which was varied as a function of E_γ to compensate for the slowing of the nuclei in the target. Events from individual channels were then sorted into seven $E_\gamma - E_\gamma$ matrices. Each matrix contained coincidences of detectors in a narrow angular segment (relative to the beam axis) and any other detector. The individual angular segments consist of groups of rings of detectors in the GAMMASPHERE array at average angles $\bar{\theta} = 29.9^\circ, 52.9^\circ, 74.3^\circ, 90.0^\circ, 105.1^\circ, 127.1^\circ, 150.1^\circ$. The matrices were gated on the energies of in-band transitions of the SD bands, and one-dimensional spectra were projected onto the axis containing counts from the angular segment, $\bar{\theta}$. The centroids of the SD band transitions (E_γ) were measured in the resultant spectra. Subsequently, a residual Doppler shift (β_{res}) was fitted to the seven ($E_\gamma, \bar{\theta}$) pairs (for each transition in the SD bands), using the expression $E_\gamma = E_\gamma^0 \sqrt{1 - \beta_{res}^2} / (1 - \beta_{res} \cos(\bar{\theta}))$, by a least-squares procedure. The residual and applied Doppler shifts of individual transitions add relativistically to obtain an average recoil velocity β , which is expressed as a fraction of the initial recoil velocity, $\beta / \beta_0 \equiv F(\tau)$. A one dimensional spectrum resulting from the sums of single gates on the SD band in ^{84}Zr is shown in Fig. 1(a). Inserts 1(b) and 1(c) contain spectra gated on two separate angular segments of detectors.

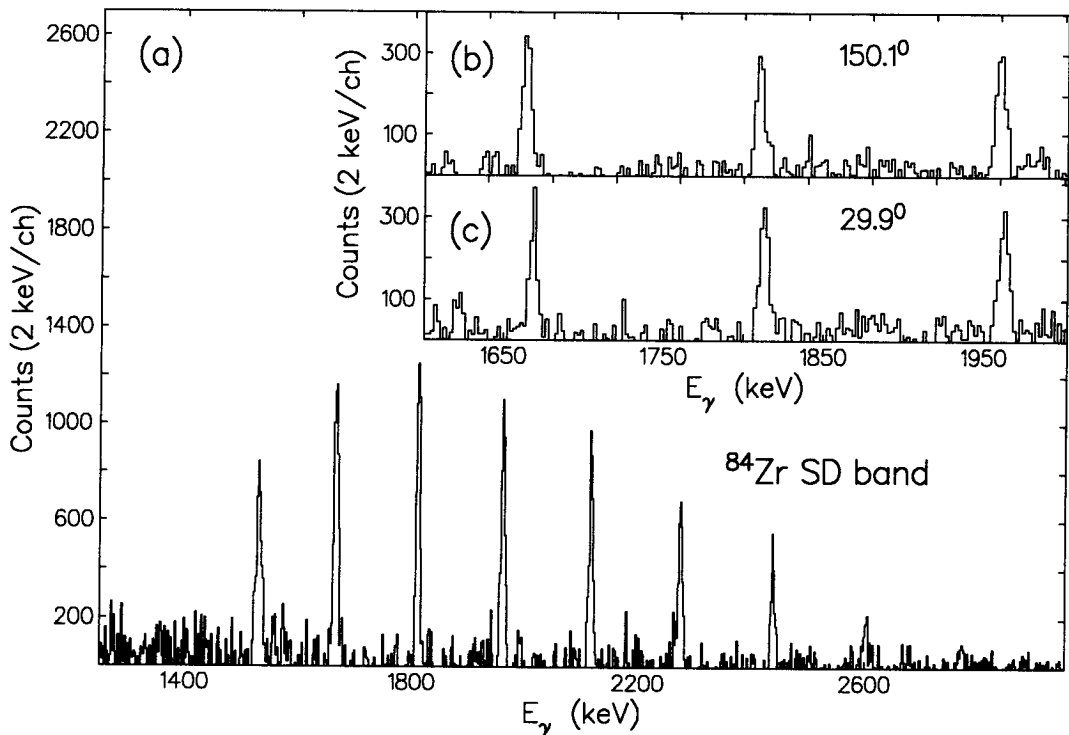


FIGURE 1. A spectrum resulting from the sums of clean single gates on in-band transitions of the SD band in ^{84}Zr is shown in panel (a). Spectra single gated on the ^{84}Zr SD band on all coincidences with angular segments of 15 detectors at 150.1° and 29.9° (relative to the beam axis) are shown in panels (b) and (c) respectively.

The average lifetimes of the SD bands were measured by fitting calculated fractional Doppler shift curves to the measured $F(\tau)$ curves for each SD band, using the Doppler-shift attenuation method described in Ref.

[5,8]. In this method, the decay times of the states in the SD bands are related to the velocity of the recoiling nuclei as they slow down in the target. Side feeding was modeled based on measured intensity patterns, and a constant Q_t was fitted to all levels in-band and those in the side-feeding cascades. Thus, side-feeding times were assumed to be equal to those of preceding in-band transitions.

Absolute values obtained from this method contain systematic errors which result from the electronic and nuclear stopping power estimates that are used to calculate the slowing of the recoiling nuclei in the target foil, and from the measured thickness of the target foil and backing, which are known approximately. For the time scales and therefore the velocities involved in the decay of the SD states the electronic stopping dominates. This reduces large systematic errors due to nuclear stopping when the recoiling species slow down in the same media of the target and the Au backing. Thus, accurate and meaningful comparisons of the extracted values could be made.

RESULTS AND DISCUSSION

The $F(\tau)$ curves extracted from the backed target experiment displayed a significant improvement in sensitivity to the lifetimes of the SD bands compared to those values extracted from thin target experiments. An example of this is shown in Fig. 2, where $F(\tau)$ curves are compared for the yrast SD band in ^{81}Sr . The fitted curve to the extracted $F(\tau)$ values of the SD band in ^{81}Sr represents the best fit performed in this analysis, in contrast, the fit to the SD band in ^{84}Zr was the least favorable fit obtained. It is likely that the poorer fit results from the reduced sensitivity to the shorter decay times of the states in the SD band in ^{84}Zr .

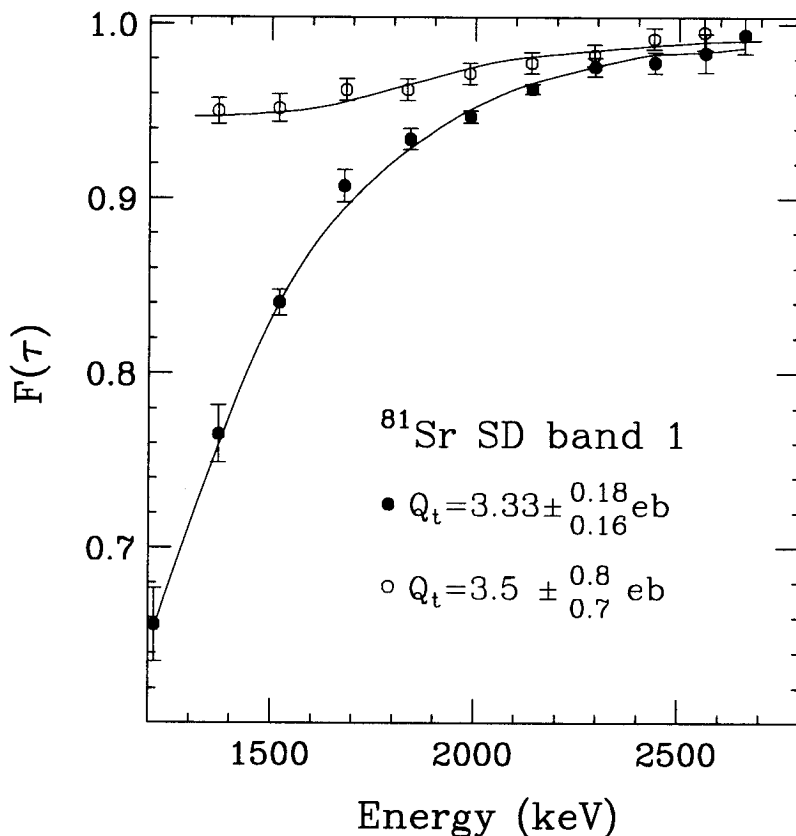


FIGURE 2. Fractional Doppler-shifts $F(\tau)$ of the yrast SD band in ^{81}Sr obtained in the backed target experiment (solid circles) are compared to those from an earlier work [5] using a thin target. The fractional shift of the last transition in the band from the backed target experiment is reduced to 65%, versus 95% obtained from the thin target experiment.

The Q_t of the SD bands in the $^{80-83}\text{Sr}$ isotope chain are shown in Fig. 3(a) and those of the SD bands

in ^{82}Sr , ^{83}Y , and ^{84}Zr in panel (b). Previously measured values, and values deduced from previous intruder orbital assignments are shown for comparison.

Intruder orbital assignments indicate a rise in deformation for the SD bands in the $^{80-83}\text{Sr}$ isotopes upon the addition of neutrons to the ^{80}Sr core, and previous experimental evidence displays a similar pattern in the $^{80-82}\text{Sr}$ cases, suggesting partial confirmation of that trend. In the case of the SD bands in the ^{82}Sr , ^{83}Y and ^{84}Zr isotone chain, large values are predicted in all cases from intruder orbital calculations, and those values are satisfactorily reproduced by previous experimental values (within the large experimental uncertainties), possibly suggesting the same intruder orbital configurations for these structures.

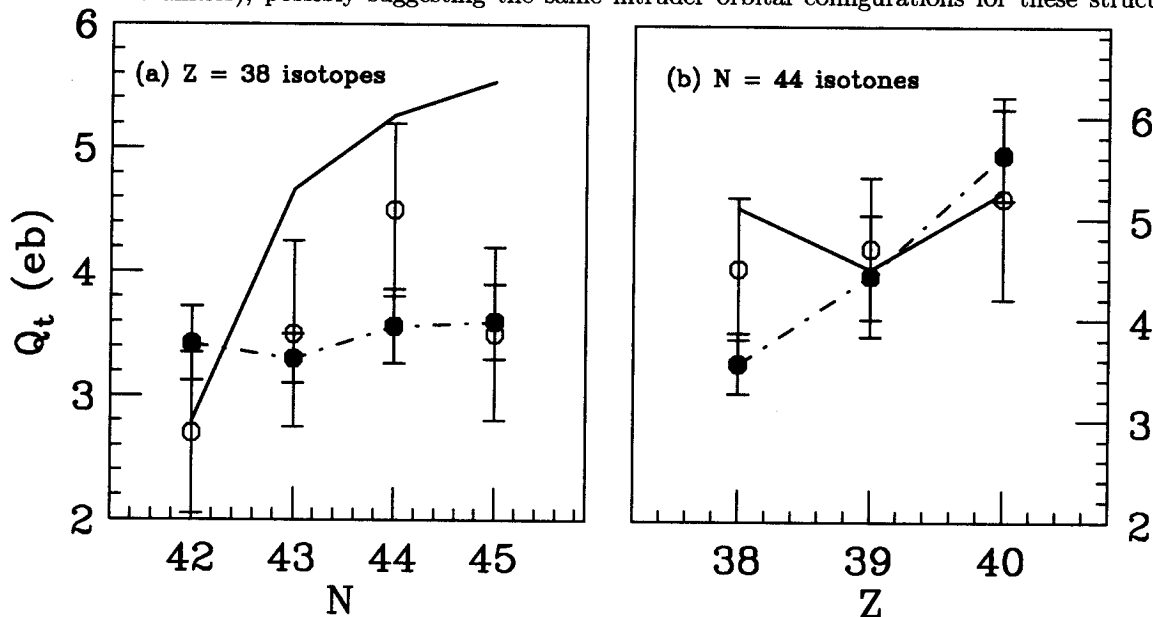


FIGURE 3. The average transition quadrupole moments obtained for the yrast SD bands in $^{80-83}\text{Sr}$ are shown in panel (a), and those values obtained for the ^{82}Sr , ^{83}Y , and ^{84}Zr cases are displayed in panel (b). Solid circles represent results obtained in this work. Open circles which represent results obtained in previous works and a solid line representing values estimated from intruder orbital calculations are shown for comparison.

However, the present results allow accurate comparisons which reveal significantly different trends. A nearly constant transition quadrupole moment is observed for the yrast SD bands in $^{80-83}\text{Sr}$, and a rise in Q_t is observed for the SD bands in ^{82}Sr , ^{83}Y , and ^{84}Zr . These new results suggest similar intruder-orbital configurations for the SD bands in the $^{80-83}\text{Sr}$ isotope chain, and the significant rise in deformation of the SD bands in the $N = 44$ isotones possibly indicates that the additional protons in the ^{83}Y and ^{84}Zr structures occupy deformation-driving $h_{11/2}$ orbitals which the SD band in ^{82}Sr does not. This is in contrast to a previous work [6], in which the SD bands in ^{82}Sr and ^{84}Zr were reported to have similar deformations, and consequently were interpreted to possess the same configuration.

Theoretical predictions from intruder-orbital assignments (based primarily on the $\mathcal{J}^{(2)}$ character of these bands) predict large deformations for all SD bands except the yrast SD band in ^{80}Sr , showing good agreement with the experimental Q_t values for the ^{83}Y and ^{84}Zr cases. However, the yrast SD bands in $^{81-83}\text{Sr}$ possess moderate Q_t values, contrary to a predicted rise in deformation from intruder orbital assignments, and a larger deformation is observed than that predicted for the ^{80}Sr case. Earlier theoretical calculations indicate that various bands may be populated at the spins considered, and that there are not unique solutions that can be selected based on the extracted $\mathcal{J}^{(2)}$ values only. Therefore, the transition quadrupole moment is a more robust quantity which can lead to a better interpretation of the intruder orbitals involved. In Ref. [13], a class of solutions are presented for the ^{80}Sr case, covering a wide range of deformations and spins. Similarly, various solutions are mentioned for the $^{81,82,83}\text{Sr}$ cases in previous works. However, those solutions are not presented in sufficient detail to make new assignments to accommodate the newly measured Q_t values of the SD bands in $^{80-83}\text{Sr}$.

SUMMARY

We have presented an experiment in which the relative transition quadrupole moments of the SD bands in $^{80-83}\text{Sr}$, $^{80-83}\text{Y}$, and $^{80-83}\text{Zr}$ have been accurately measured. The use of a backed target has demonstrated a significant improvement in the sensitivity to the lifetimes of these structures, and the use of the same experimental conditions (primarily the use of the same target and backing) have allowed accurate comparison of these results. Previous trends in the deformation of the SD bands in these nuclei have been discussed, and a new well-defined trend has been presented. Large discrepancies have been shown between the present results and those derived from previously assigned intruder orbital configurations for the SD bands in $^{80-83}\text{Sr}$ suggesting new theoretical calculations are necessary to interpret the configuration of these structures.

ACKNOWLEDGEMENTS

The work at Washington University is supported in part by the U.S. Department of Energy (DOE), Division of Nuclear Physics under grant No. DE-FG02-88ER-40406. Oak Ridge National Laboratory is managed by Lockheed Martin Energy Research Corp. for the US DOE under contract DE-AC05-966OR22464. The work at Lawrence Berkeley National Laboratory is supported in part by the U.S. DOE, Division of Nuclear Physics under grant No. DE-AC03-76SF00098. The U.S. National Science Foundation provides support for the work at Florida State University under grant No. PHY-9210082. The authors are grateful to A. Lipski for making the target for this experiment.

REFERENCES

1. C. Baktash *et al.*, Phys. Rev. Lett. **74**, 1946 (1995).
2. D. R. LaFosse *et al.*, Phys. Lett. B **354**, 34 (1995).
3. H.-Q. Jin *et al.*, Phys. Rev. Lett. **75**, 1471 (1995).
4. D. G. Sarantites *et al.*, Phys. Rev. C **57**, 1 (1998).
5. M. Devlin *et al.*, Phys. Lett. B **415**, 328 (1997).
6. C.-H. Yu *et al.*, Phys. Rev. C **57**, 113 (1998).
7. D. Rudolph *et al.*, Phys. Lett. B **389**, 463 (1996).
8. B. Cederwall *et al.*, Nucl. Instr. and Meth. A **354**, 591 (1995).
9. H.-Q. Jin *et al.*, to be published, private communication.
10. D. G. Sarantites *et al.*, Nucl. Instr. and Meth. A **381**, 418 (1996).
11. M. Devlin *et al.*, Nucl. Instr. and Meth. A **383**, 506 (1996).
12. C. E. Svensson *et al.*, Nucl. Instr. and Meth. A **396**, 228 (1996).
13. W. Nazarewicz *et al.*, Nucl. Phys. A **435**, 397 (1985).